IOP Publishing Journal of Physics D: Applied Physics
J. Phys. D: Appl. Phys. **53** (2020) 425103 (7pp) https://doi.org/10.1088/1361-6463/ab98c2

Elucidating the capability of electron backscattering for 3D nano-structure determination

H Trombini[1,2], M Vos[2], S Reboh[3] and P L Grande[1]

[1] Instituto de Física, Universidade Federal do Rio Grande do Sul, Av. Bento Gonçalves 9500, CP 15051 Porto Alegre–RS, Brazil
[2] Electronic Materials Engineering, Research School of Physics, Australian National University, Canberra, Australia
[3] CEA-LETI, MINATEC Campus, F-38054 Grenoble, France

E-mail: henrique.trombini@ufrgs.br

Received 17 March 2020, revised 29 May 2020
Accepted for publication 2 June 2020
Published 29 July 2020

Abstract

Reflection electron energy loss spectroscopy (REELS) is well established for the study of homogeneous materials with flat surfaces. Here we extend the use of this technique to nano-structures consisting of silicon and silica and show that the experimentally-observed peculiar dependence of the REELS spectra on the sample orientation can be reproduced by Monte Carlo simulations using the known sample morphology. A sample with a 3D structure, resembling those found in FinFET transistors, was analyzed through electron Rutherford backscattering (ERBS, revealing the mass of the atoms near the surface) and REELS (revealing the electronic structure). ERBS/REELS spectra were taken at two incoming electron energies (5 and 40 keV) and in two experimental geometries with the component of the outgoing propagation direction along the surface being either parallel or perpendicular to the fins. The measured spectra were different for the two geometries due to attenuation effects within the fins, especially at 5 keV where the inelastic mean free path is of the order of the fin dimensions. This means that the 3D structure induces shadowing effects which suppress the elastic peaks and enhanced the inelastic signal. A Monte Carlo code was used to simulate multiple elastic and inelastic interactions of the electrons with these 3D structures and was indeed able to reproduce these experimental results, including the shadowing effects. A sub-angstrom layer of Au was evaporated on the sample and the changes induced by the Au layer were dependent on the orientation of the fins and were again reproduced by the simulation.

Supplementary material for this article is available online

Keywords: electron Rutherford backscattering, reflection electron energy loss spectroscopy, electron transport in matter, 3D nano-structures

(Some figures may appear in colour only in the online journal)

1. Introduction

The analysis of near-surface structures of samples by ion-beam and electron-spectroscopic techniques has been a mainstay of material science. In particular, the variation of elemental composition with depth (depth profiling) and homogeneity of coverage (e.g. island versus layer-by-layer growth mode) have been studied extensively (see e.g. [1]).

Modern nano-science technology introduces applications of more complex morphologies and hence surface-analytical techniques have to evolve to be able to characterize these surface structures as well. One example that attracted attention

recently is the analysis of 'core–shell nanoparticles' where the center region of the particle has a different composition of the shell, and extracting the shell, core dimensions and composition is then required [2, 3]. Another interesting case is when the surface is artificially structured in one direction in a different way from the perpendicular direction. A technological example of such a structure is 3D fin field effect transistors (FinFET), nowadays widely used in micro-electronics. Understanding of how such an artificial anisotropy affects surface-sensitive techniques, and, consequently, how we can use these techniques to characterize such a surface, is an important question to address [4–6].

Here we investigate how FinFET-like structures affect reflection electron energy loss spectroscopy (REELS) measurements using incoming electrons with energy between 5 and 40 keV. At 40 keV, the recoil effect makes it possible to determine the mass of the scattering atom for the part of the spectrum called the 'elastic peak' where no inelastic excitations are created. In this regard, REELS at high energies resembles (ion-based) Rutherford backscattering and hence measurements focusing on the elastic peak only are usually referred to as electron Rutherford backscattering (ERBS). Thus, the elastic peak probes the near-surface elemental composition.

Away from the elastic peak, the structures are determined by the electronic structure (in particular the associated 'energy loss function' (ELF)) of the various layers that compose the sample morphology/geometry. Determination of the ELF is the focus of REELS experiments of homogeneous samples. In our case, the sample consists out of crystalline Si (the fins and substrate) as well as a partially buried SiO_2 layer. The relative intensity of these contributions depends on attenuation, which, as we will see, depends on the orientation of the fins. By decreasing the energy of the probing electron, one can decrease the inelastic mean free path (IMFP) and hence increase the strength of these anisotropic attenuation effects. However, at lower energies, one does not resolve the variation in recoil losses of the different elements any more.

The influence of the IMFP on the spectrum also underpins the interpretation of XPS measurements of the surface structure. The experiments described here have conceptual overlap with both RBS and XPS, and hence the understanding of these REELS experiments provides a bridge linking the interpretation of both techniques.

Measurement of these anisotropic effects only becomes an effective surface characterization tool if one has a model that describes the anisotropy of the REELS spectra for a given sample. For this we use a Monte Carlo program that describes the sample in terms of voxels, i.e. it can take into account the three-dimensional structure of the sample [7, 8]. In this approach, the energy loss contribution is just determined by the local sample composition. The validity of this approach is not completely obvious. The energy loss is (within the framework of the dielectric theory) a consequence of the polarization of the environment of the propagating charge. If the environment is inhomogeneous, the local approach may fail. Examples of such deviations are surface and interface plasmons that cannot be described in such a simple local approximation [9].

The aim of this paper is to demonstrate that the orientation of the fins affect the measurement and that the local approximation, for the incoming energy values used here, is good enough to resolve the main effects of the sample anisotropy on the observed ERBS/REELS spectra.

2. Experimental procedure

2.1. Sample description

To demonstrate the capability of electron backscattering to characterize 3D nano-structures, we used a fin-like structure as illustrated in figure 1(a). The starting point to obtain this sample was a silicon-on-insulator (SOI) wafer with a 25 nm buried oxide layer and a surface Si layer of 50 nm. A part of the wafer (6 mm long, 2 mm wide) was patterned using lithography and the top Si layer was selectively etched away down to the oxide layer to obtain fin-like structures of 50 nm height (H_{fin}), 20 nm width (W_{fin}) and fin-pitch (periodicity) of 65 nm. This part of the sample had a distinct blue color facilitating the alignment of the 'FinFET' part of the sample with the electron beam in the spectrometer. The area of the sample without the fin-like structure will be referred to only as SOI. A 3 nm native oxide was assumed to cover the surface of all fin structures.

2.2. ERBS/REELS

The fin-like structures and the SOI were measured at the high-energy electron scattering spectrometer at the Australian National University (ANU) using an incoming beam with energies of 5 and 40 keV (beam diameter 0.2 mm), corresponding to the minimum and maximum energies achieved by our system. After the first set of measurements a gold deposition of $\approx 4.5 \times 10^{14}$ atoms per cm^2 (using the density of Au metal this corresponds to a 0.076 nm thick Au layer) was performed and the assumed Au distribution is illustrated in figure 1(b). The Au thickness was measured after the REELS experiment using the (ion) Rutherford backscattering technique [10].

The measurements of the fin-like structures were performed in two geometries where the outgoing electron have different paths inside the material. The incoming beam was always along the surface-normal but two exit trajectories were selected: crossing ($\varphi = 90°$) and along ($\varphi = 0°$) the fin, as illustrated in figure 1(c). The beam diameter of 0.2 mm allows us to perform the measurement over more than three thousand structures, being highly representative in a statistical meaning. Figure 1(c) also shows the incoming and outgoing paths of the backscattered electrons at the top of the fin and at the bottom between the fins for both geometries. The main difference between $\varphi = 0°$ and $\varphi = 90°$ is expected for those electrons backscattered from between fins. For the outgoing trajectory with $\varphi = 90°$ the electrons backscattered from in between the fins have to transverse at least one fin, while for $\varphi = 0°$ this is not required.

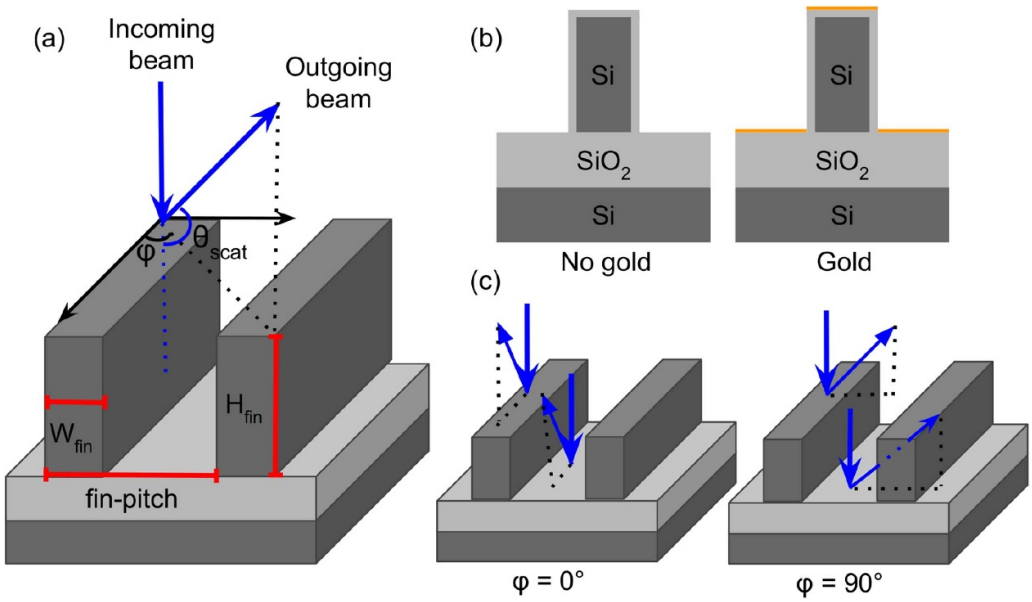

Figure 1. (a) Sample illustration and experimental setup indicating the φ angle between the incoming and outgoing beam in relation to the sample surface. (b) Front view of the fin structure indicating the SiO_2 overlayer and the gold deposition. (c) The sample was fixed in two different positions which allows the measurement of outgoing electron paths along ($\varphi = 0^\circ$) and crossing ($\varphi = 90^\circ$) the fins.

3. Results and discussion

3.1. Reference spectra

To understand REELS spectra of these structured samples, it is useful to first consider the spectra of pure Si and SiO_2 and Si with less than a monolayer of Au at its surface. The influence of recoil losses and the different shapes of the energy loss spectra can be seen in figure 2. The incoming electron beam with $E_0 = 40$ keV energy was incident along the surface normal. The spectra were aligned such that the main elastic peak (corresponding to Si) is at the calculated recoil energy, which is 2.77 eV for 40 keV electrons scattering over 135° from Si. The ERBS part of the spectra indicated in figure 2 is associated with electrons that have been backscattered without losing energy due to electronic excitations. On the other hand, the REELS part (energy losses larger than ≈ 6 eV) carries the information of the electrons that created also electronic excitations with an energy loss distribution that depends on the target dielectric function. For the pure Si target, the plasmon peak emerges at $\sim$20 eV, which corresponds to the sum of the recoil loss (2.77 eV) plus the plasmon excitation energy ($\sim$17 eV), but for SiO_2 the energy loss has a broader distribution. Note that the Au deposited at the surface of Si does not noticeably affect the REELS spectrum, which means that, for this amount of Au, basically no electrons are scattered inelastically in the Au. This is because the IMFP is much greater than the Au thickness. That means that the Au signal is completely located in the ERBS part.

3.2. Simulations

The experimental results were compared to simulated ones obtained through the Monte Carlo program named PM3 [7, 8]. PM3 simulates the interactions of ions [6] and electrons [11] with matter. For enhanced computational efficiency, PM3 uses a variation on the trajectory reversal approach [12] to connect incoming and outgoing electron trajectories. These trajectories are constructed by first simulating two sets of trajectories: one set starting from the gun, and one set starting from the analyser. The position, energy, and path traveled by the electrons during these trajectories are stored. The contribution of a specific incoming and outgoing trajectory combination from an atom A at position x, y, z is proportional to the differential elastic scattering cross section of atom A at the scattering angle between the incoming and (time-reversed) outgoing electron trajectory and the concentration of atom A at x, y, z. Energy losses due to inelastic excitation and atomic recoils were calculated using standard Monte Carlo techniques (see e.g. [13]) and the mentioned dielectric function. The dielectric function of Si, and SiO_2 were taken from [14]. The differential elastic cross sections were calculated using ELSEPA [15] for the nominal incoming energy. ELSEPA is a FORTRAN 77 code that allows the calculation of elastic scattering of electrons and positrons by atoms, positive ions, and molecules. PM3 describes the sample by voxels organized in a matrix format, which may represent any complex structure consisting of a number of compounds [16]. In practice, the voxel was a cube with 1 nm length. The voxel model used here was very similar to the one used to describe the ion-scattering results from similar FinFETs [6]. As the Au layer, when present, was much less than 1 nm, it was simulated as a 1 nm thick SiO_2Au_x layer with $x = 0.2$ for the amount of Au present as measured by RBS. It was assumed that the loss function of this SiO_2Au_x alloy was the same as that of pure SiO_2. PM3 assumes an amorphous target, i.e. the contribution from different atoms are added incoherently. It is thus important to avoid in the experiment geometries where electron diffraction plays a major role. A brief

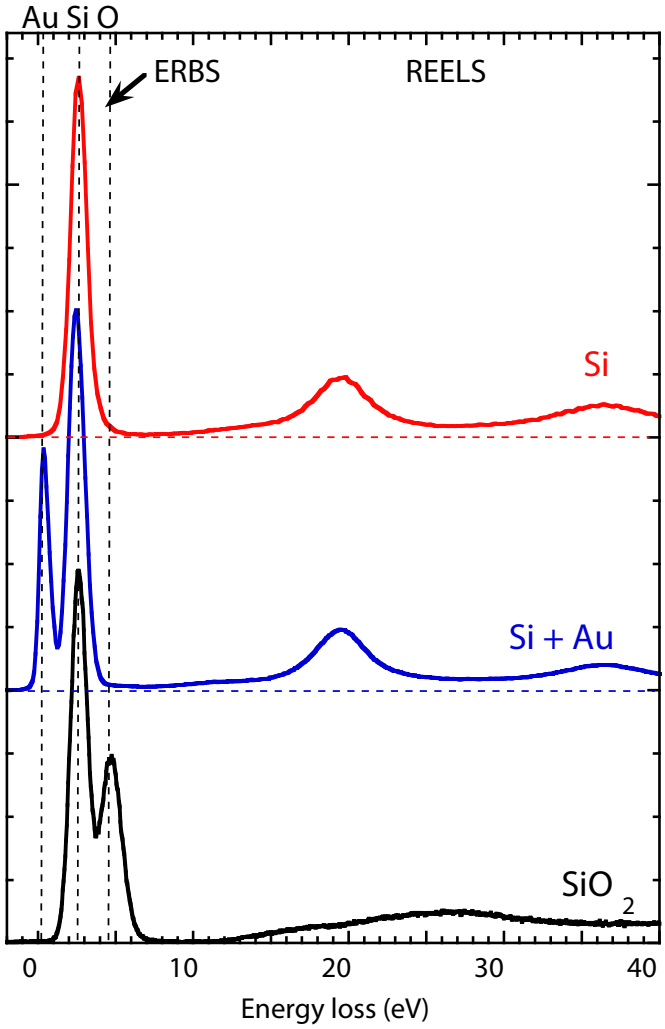

Figure 2. Typical ERBS/REELS spectra for pure Si, a monolayer of gold deposited over the pure Si and pure SiO_2. Measurements was performed with an incoming beam of 40 keV electrons normal to the sample surface and at the backscattering angle of 135°.

discussion of the diffraction effect is provided in the supporting information (stacks.iop.org/JPD/53/425103/mmedia).

3.3. Experimental ERBS/REELS results compared to simulations

The experimental (top) and simulated (bottom) ERBS/REELS spectra for the 40 keV incident beam are shown in figure 3(a). For this incoming beam energy, it was possible to separate the Si and O elastic peak as indicated in figure 3(a), as the recoil energies decrease with atomic mass. The SOI part of the sample shows much less O intensity than the FinFET part at either 0° and 90°. This is expected as the SiO_2 layer is buried for the SOI sample in contrast to the FinFET sample which has exposed SiO_2 between the fins. All data were normalized to equal height near energy losses of ∼100 eV. At such large energy loss, the signal is mainly generated from larger depths where all measurements probe pure Si, and one would not expect great changes in intensity due to the presence of a FinFET structure near the surface. Differences between measurements with the FinFET sample using the experimental geometry 0° and 90° show up in both the ERBS and REELS parts, but spectra of the SOI part of the sample were not affected by this rotation of the sample. The O elastic peaks is more intense for the FinFET at 0° than for the FinFET at 90°. At 90° the outgoing trajectory of electrons scattered from O always have to transverse the fin (and hence are attenuated), whereas this is not necessary for the 0° orientation. We refer to this as a 'shadowing effect'. For the inelastic part, the contribution of the SiO_2 plasmon to the spectrum is more significant for the FinFET part. It has a broad maximum at 10 eV larger energy loss than the Si plasmon. Thus, the SiO_2 loss contribution fills in the valleys between the Si plasmon losses and hence makes the Si plasmons stand out less for the FinFET sample.

The PM3 simulation reproduces almost all these tendencies very well. The simulations were also normalized to equal intensity near 100 eV energy loss. The O elastic peak behaves very similarly to the experimental one, i.e. it is smallest for the SOI spectrum and largest for the 0° FinFET orientation. The difference in shape of the loss spectrum, a consequence of the different relative contributions of losses in

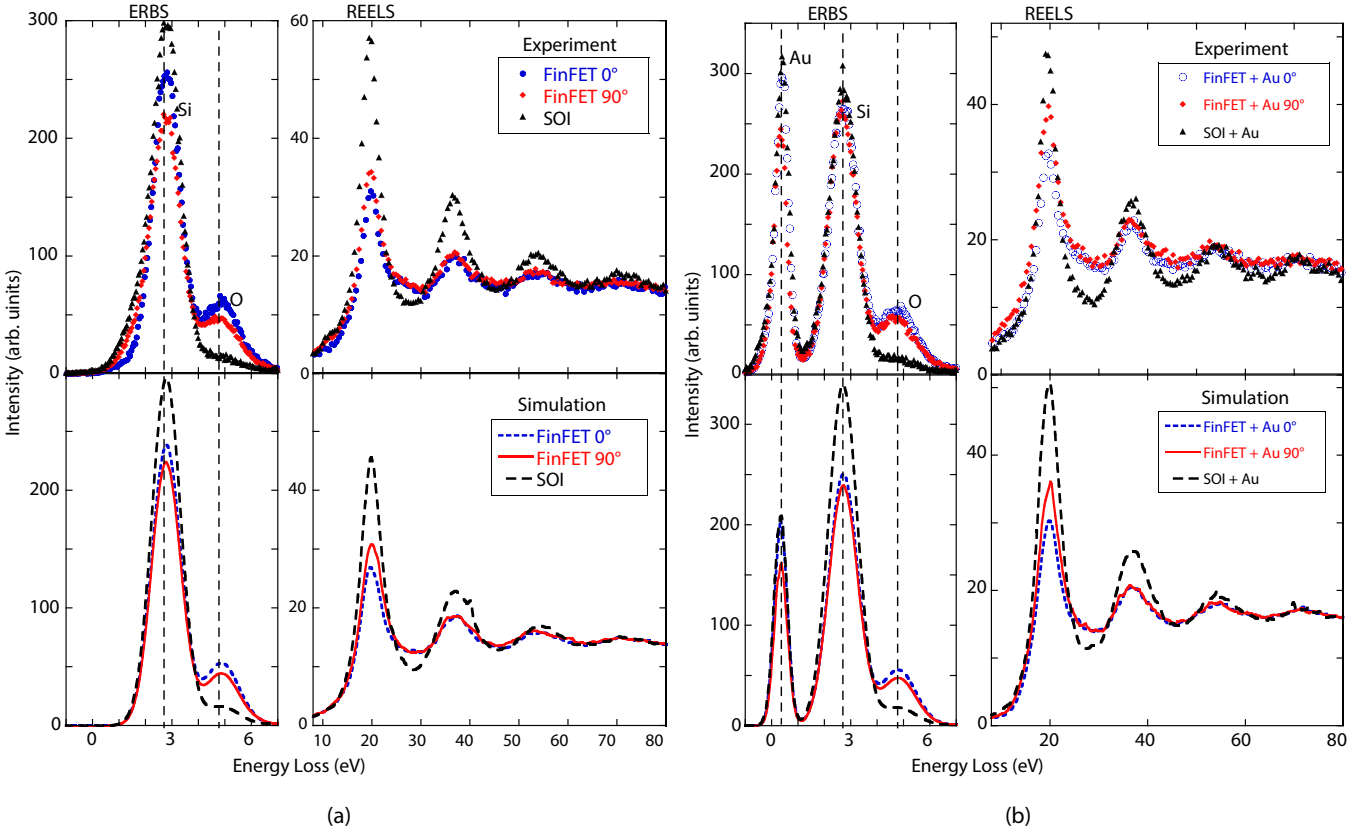

Figure 3. 40 keV ERBS/REELS experimental (top) and simulated (bottom) spectra for the sample without gold (a) and with gold (b). The dots and lines represent the experimental and simulated data, respectively. Blue, red and black correspond respectively to the measurements performed in the FinFET at 0°, FinFET at 90° and SOI samples.

Si and SiO_2, is reproduced very well. The main difference is that the Si plasmon is somewhat narrower (and hence more intense) in the experiment than in the simulation. The simulations were performed with 5×10^8 electron trajectories and each simulation took at least 15 minutes. There are visible differences in the spectra for variations in nominal dimensions greater than about 10% for the W_{fin} and H_{fin} and 20% for the fin-pitch.

After Au evaporation (figure 3(b)), an additional elastic peak is observed very close to zero energy loss, as expected for electrons scattered from the heavy Au atoms. This elastic peak is of similar strength for the SOI spectra and the 0° FinFET orientation but the Au peak is slightly weaker for the 90° FinFET orientation. As the spectra are from the same sample, the Au thickness does not vary. The reduction in Au intensity at 90° is again due to 'shadowing' of the part of the Au atoms that is located in the trenches. For Au on the SOI part and for the 0° FinFET orientation, electrons scattered from Au do not need to transverse the fins and hence attenuation should not occur. Those electrons scattering inelastically from Au in the between fins will contribute to the Si plasmon. Indeed the evaporation of Au enhances the Si plasmon for the 90° FinFET orientation. Moreover, the Au elastic peak is not affected by the Kikuchi effect since it is polycrystalline. Therefore, it was used to analyze possible Kikuchi effects in the Si signal as described in the supporting information.

Again the simulations reproduce the experimental trends well. The main discrepancy now is that the Au peak is less intense in the simulation that the experiment. Note that the amount of Au present was determined from ion-RBS and not a free parameter. For the experimental geometry used (incoming beam along surface normal), the Si intensity can be increased considerably due to channeling effects of the incoming beam, and we assume that is also the cause of the discrepancy here.

The shadowing effect is directly determined by the sample dimensions (H_{fin}, W_{fin} and fin-pitch) and the IMFP. By decreasing the electron beam energy, one reduces the inelastic mean free path and thus increases the shadowing effect. However, at much lower energies, one looses the elemental separation in the elastic peak. Results of experiments with $E_0 =$ 5 keV are shown in figure 4, again normalized near 100 eV energy losses. At this energy, we can no longer separate the contribution of each element in the ERBS spectrum, which means that the elastic peak is related to the Si plus O signals and Si plus O plus Au signals in figures 4(a) and (b), respectively. Note that for the gold sample, the elastic peak is twice as intense. Thus, for all three measurements, the presence of Au is evident from the anomalous height of the elastic peak, relative to the energy loss part of the spectrum. In this way, semi-quantitative information of the amount of Au present at the surface can be obtained, even when the elastic peak recoil losses are not resolved.

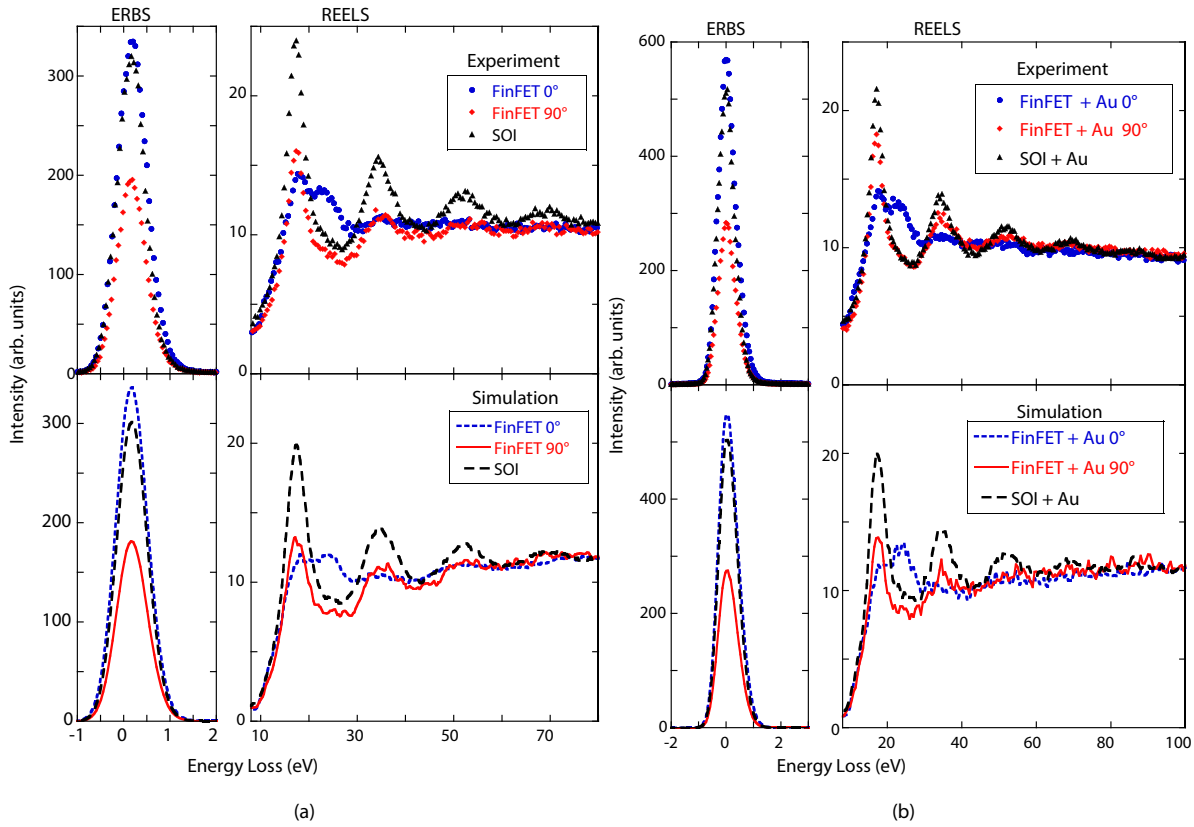

Figure 4. 5 keV ERBS/REELS experimental (top) and simulated (bottom) spectra for the sample without gold (a) and with gold (b). The dots and lines represent the experimental and simulated data, respectively. Blue, red and black correspond respectively to the measurements performed in the FinFET at 0°, FinFET at 90° and SOI samples.

The IMFP for 5 keV electrons (88 Å for Si and 105 Å for SiO_2) is ∼5 times smaller than for 40 keV electrons (485 Å for Si and 582 Å for SiO_2) [17]. Thus, most of the electrons backscattered between fins will produce electronic excitations in the fins along the outgoing path to the analyzer. This is clearly demonstrated in figure 4 where the elastic peak for the FinFET at 90° is almost half of the elastic peak for the FinFET at 0°. The shadowing effect can also be easily seen in the REELS spectra. The electrons lose energy mainly in the SiO_2 between fins for the FinFET at 0° since our fin-like structures have $W_{fin} = 20$ nm and fin-pitch = 65 nm, and thus 45 nm (i.e. 70% of total surface area) of exposed SiO_2. For this reason, the REELS spectra for the FinFET at 0° shows an energy loss distribution similar to the SiO_2 plasmon shown in figure 2. For the FinFET at 90°, the REELS spectrum becomes much more similar to the Si spectrum shown in figure 2, which means that the electrons backscattered elastically from the Si and O atoms between fins produce electronic excitations in the silicon of the fins along the outgoing path. This result shows that the variation of the incoming beam energy produces strong changes in the ERBS/REELS spectra.

The shadowing effect is related to the IMFP, and consequently to the beam energy and the fin-like structure dimensions (due to the total distance traveled by the electron before being detected) which induce changes in the energy loss spectrum. For an electron beam with low energy, the shadowing effect can arise even in planar samples with roughness. This approach combined with the PM3 code shows the possibility of investigation of 3D structures, including its dimensions and elemental composition. Examples of such 3D structures include nanowires with periodic structure and the determination of high-Z elements in nanoparticles even with small concentrations.

4. Conclusions

In this paper, we have shown the influence of 3D structures (fin-like structures) on the ERBS/REELS spectrum. Two experimental geometries were applied in order to get a different outgoing path for the backscattered electron inside the structure. It has been shown that the energy dependence of the IMFP plays a fundamental role over the ERBS/REELS spectra variations as well as the dimensions of the 3D structure. The shadowing effects give information of the 3D structure as they induce changes on the elastic and inelastic regions of the spectrum. These changes of the ERBS/REELS spectra combined with the PM3 code allow the investigation of the dimension and geometry of 3D structures. This procedure could be used in other nanostructures as, for example, nanoparticles and nanowires. Also, we demonstrate that a quantification of the influence of diffraction on these measurements is also necessary (supporting information). These results open up new possibilities to 3D structures characterization through electron beams.

Acknowledgments

We are indebted to the Brazilian National Council for Scientific and Technological Development (CNPq, 160018/2019-6) for the partial support of this research project. The authors want to thank Hagege Abay Weldu for help with measurements, Robert G Elliman for the RBS measurement and Gabriel G Marmitt for the PM3 code.

ORCID iDs

H Trombini https://orcid.org/0000-0002-7254-4774
M Vos https://orcid.org/0000-0003-2668-9216

References

[1] Woodruff D P 2016 *Modern Techniques of Surface Science* (Cambridge: Cambridge University Press)
[2] Chudzicki M, Werner W S M, Shard A G, Wang Y-C, Castner D G and Powell C J 2015 Evaluating the internal structure of core-shell nanoparticles using x-ray photoelectron intensities and simulated spectra *J. Phys. Chem.* C **119** 17687
[3] Sanchez D, Moiraghi R, Cometto F P, Pérez M A, Fichtner P and Grande P L 2015 Morphological and compositional characteristics of bimetallic core@shell nanoparticles revealed by MEIS *Appl. Surf. Sci.* **330** 164
[4] Laricchiuta G, Vandervorst W, Vickridge I, Mayer M and Meersschaut J 2019 Rutherford backscattering spectrometry analysis of InGaAs nanostructures *J. Vac. Sci. Technol.* A **37** 020601
[5] Min W J, Kim J, Park K, Marmitt G, England J and Moon D W 2019 Determination of dimension and conformal arsenic doping profile of a fin field effect transistors by time-of-flight medium energy ion scattering *Anal. Chem.* **91** 9315–22
[6] Trombini H *et al* 2019 Unraveling structural and compositional information in 3d finfet electronic devices *Sci. Rep.* **9** 1–7
[7] Marmitt G 2017 Metal oxides of resistive memories investigated by electron and ion backscattering *PhD Thesis* Universidade Federal do Rio Grande do Sul
[8] Marmitt G G Powermeis Simulation Code (http://tars.if.ufrgs.br/)
[9] Raether H 1988 Surface plasmons on smooth and rough surfaces and on gratings *Springer Tracts in Modern Physics* (New York: Springer)
[10] Chu W K, Mayer J W and Nicolet M A 1987 *Backscattering Spectrometry* (New York: Academic)
[11] Vos M, Grande P L and Marmitt G G 2018 The influence of shallow core levels on the shape of REELS spectra *J. Electron Spectrosc. Relat. Phenom.* **229** 42–6
[12] Werner W 2005 Trajectory reversal approach for electron backscattering from solid surfaces *Phys. Rev.* B **71** 115415
[13] Dapor M 2010 *Electron-Beam Interactions With Solids: Application of the Monte Carlo Method to Electron Scattering Problems* (Berlin: Springer)
[14] Da B, Sun Y, Mao S F and Ding Z J 2012 Systematic calculation of the surface excitation parameters for 22 materials *Surf. Interface Anal.* **45** 773–80
[15] Salvat F, Jablonski A and Powell C J 2005 ELSEPA Dirac partial-wave calculation of elastic scattering of electrons and positrons by atoms, positive ions and molecules *Comput. Phys. Commun.* **165** 157–90
[16] Sortica M A, Grande P L, Machado G and Miotti L 2009 Characterization of nanoparticles through medium-energy ion scattering *J. Appl. Phys.* **106** 114320
[17] Tougaard S 2002 QUASES-IMFP-TPP2M code for the calculation of the inelastic electron mean free path, Version 2.2 (www.quases.com)